

Linear Discrete Control of Rössler System based on Circuits

Juan S. Cárdenas R.

Student

Universidad EAFIT

Medellín, Colombia

jscardenar@eafit.edu.co

David Plazas E.

Student

Universidad EAFIT

Medellín, Colombia

dplazas@eafit.edu.co

Abstract—In this work, the Rössler system is studied: a short introduction about the history of the system is given, as well as some state-of-the-art applications; a circuit implementation is presented based on the literature and translated to a state equation. The first part of this document is focused on give some basic theory, concepts and procedures to design a successful digital linear control system mainly for achieving absolute stability and remove steady-state error. This work treats with discrete PID controllers and discrete linear feedback controllers; these control system are then applied to the nonlinear Rössler system and then an uncertainty analysis is performed to find intervals where the controllers work properly.

Index Terms—Rössler system, simulation, state equation, dynamic system, absolute stability, linearization, discrete PID controller, state feedback controller, tuning methods, steady-state error, time-response properties.

I. INTRODUCTION

The system in study was proposed by O.E. Rössler in 1976, as a simplified model with shape and behavior similar to spirals in Lorenz system, which was not fully understood at the time due to the techniques known to study oscillators were not applicable to Lorenz model [1]. The Rössler equations are:

$$\begin{aligned}\dot{x} &= -y - z \\ \dot{y} &= x + ay \\ \dot{z} &= b + z(x - c)\end{aligned}\tag{1}$$

Although Rössler affirmed that the system did not have immediate physical interpretation [1], nowadays some applications can be found using the model as a mechanism and not as an abstraction of a physical system. The model presented has been used as a tool for image cryptography as it was shown by Mandal *et al.* in [2]; in further work, Laiphakpam and Khumanthem proposed improvements to Mandal's algorithm, as it is shown in [3]. On the other hand, coupled Rössler system with different inputs have been used to measure the correlation of time series, as Weule *et al.* showed in [4].

In order to bring the system to the real world, Rössler equations can be represented by a circuit, as Canals *et al.*

show in [5]. The proposed circuit is shown in Fig. 1 and can be translated to

$$\begin{aligned}a &= \frac{100k\Omega}{R_a} \\ RC\dot{x} &= -y - z \\ RC\dot{y} &= x + ay \\ RC\dot{z} &= b + z(x - c) \\ b &= V_{cc} \cdot \frac{100k\Omega}{R_b} \\ c &= \frac{100k\Omega}{R_c}\end{aligned}\tag{2}$$

In [5] they use this circuit to generate true random numbers using the output of the voltage of the node z . The nodes x and y have a fixed frequency of oscillation if the other variable is set to 0, since their rate of change are linear. In contrast, z induces chaos to the circuit, due to its nonlinear behavior. In this manner, this variable was selected to be the output as its chaotic behavior is useful to generate random numbers [5].

In this work, the question “for which values of input and R_a a linear discrete control can successfully eliminate steady-state error (e_{ss}) and mitigate the overshoot in the Rössler system?”. It is believed that it will only be able to eliminate e_{ss} for inputs near the operation point, since the Rössler attractor is highly sensitive to changes in the input; as for the parameters, given that PID controllers are robust, the controller will be able to work further from the operation point.

In section II, the dynamic system used and some theory required to design linear control systems to the Rössler equations can be found. In section IV, the analysis of the obtained results and their justification is made. Finally, the conclusions are presented in section V.

II. METHODS

A. Dynamic System

In the circuit presented, according to Canals *et al.* [5], the variables x , y and z represent the voltages through the nodes shown in Fig. 1. The RC parameter defines the system's time (in seconds), the supplied voltages are $V_{cc} = 15V$ and $V_{ss} = -15V$; R_a , R_b y R_c are resistors in $k\Omega$ used to calculate the system's original parameters, as shown in (2).

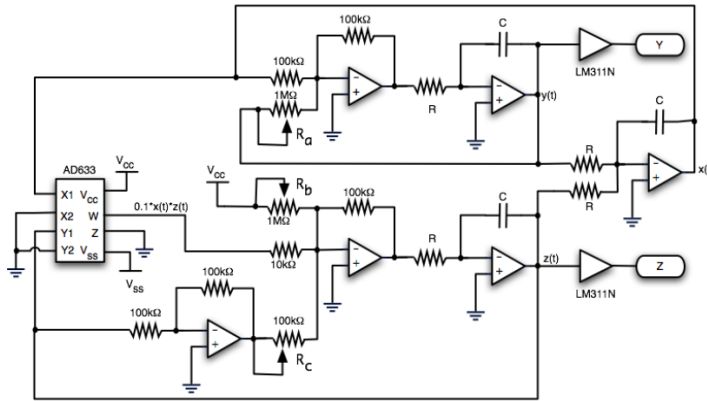


Figure 1: Rössler circuit representation [5].

The circuit can be represented through a dynamic equation, as follows:

$$\begin{cases} \dot{x}_1 = \frac{1}{RC} (-x_2 - x_3) \\ \dot{x}_2 = \frac{1}{RC} \left(x_1 + \frac{100k\Omega}{R_a} x_2 \right) \\ \dot{x}_3 = \frac{1}{RC} \left[(V_{cc0} + u(t)) \frac{100k\Omega}{R_b} + x_3 \left(x_1 - \frac{100k\Omega}{R_c} \right) \right] \\ y = x_3 \end{cases} \quad (3)$$

where y is the output and u the input; note that the parameter V_{cc} was selected as input, based on equation (2), thus we select an initial value V_{cc0} and add the input $u(t)$ in Volts. For the rest of this document, the state variable x_3 can sometimes be referred as y , since it has been chosen as the output.

B. Simulation Diagram

Using equation system (3), a simulation diagram was constructed using *Simulink*, as Fig. 2 shows.

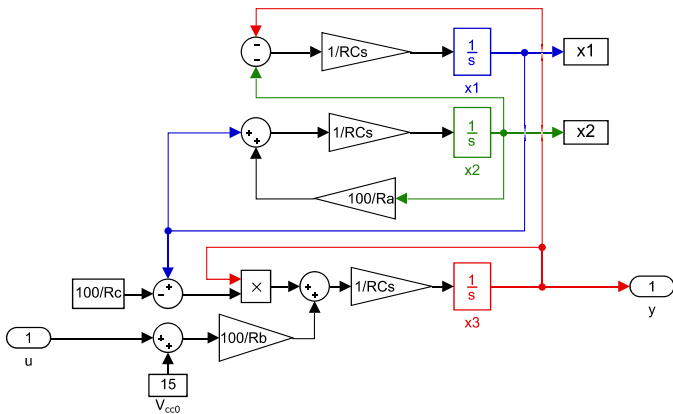


Figure 2: Simulation diagram for Rössler system.

C. Equilibrium Points

The system has the following equilibrium points:

$$\begin{cases} x_1 = \frac{100x_3}{R_a} \\ x_2 = -x_3 \\ x_3 = \frac{R_a}{2R_c} \left(1 \pm \sqrt{1 - \frac{4R_c^2[V_{cc0} + u(t)]}{R_a R_b}} \right) \end{cases} \quad (4)$$

Note the double sign in x_3 , therefore the Rössler system has two equilibrium points. These depend on both the parameters and the input $u(t)$. In this work, the same parameters studied in [6] will be used. Thus, $R_a = 500k\Omega$, $R_b = 7500k\Omega$, $R_c = 17.5439$, $V_{cc0} = 15V$, $RC = 1$ and input

$$u(t) = (1000V)H(t) \quad (5)$$

where $H(t)$ is the Heaviside or step function. Therefore, the equilibrium points for the Rössler system with said parameters are

$$\begin{aligned} P_1(x_1, x_2, x_3) &= (0.5228, -2.6140, 2.6140) \\ P_2(x_1, x_2, x_3) &= (5.1772, -25.8859, 25.8859) \end{aligned} \quad (6)$$

In this paper, the first equilibrium point P_1 will be considered for the linearization.

D. Linear Systems

1) *Continuous*: The linearized Rössler system around P_1 is given by the following state space representation:

$$\begin{aligned} \Delta \dot{\mathbf{x}} &= \begin{bmatrix} 0 & -1 & -1 \\ 1 & 0.2 & 0 \\ 2.614 & 0 & -5.1772 \end{bmatrix} \Delta \mathbf{x} + \begin{bmatrix} 0 \\ 0 \\ 0.0133 \end{bmatrix} \Delta \mathbf{u} \\ \Delta \mathbf{y} &= \begin{bmatrix} 0 & 0 & 1 \end{bmatrix} \Delta \mathbf{x} \end{aligned} \quad (7)$$

2) *Discrete*: The discrete linear system was obtained with sample time $T = 1s$, and it is presented in equation 8.

$$\begin{aligned} \Delta \mathbf{x}_{k+1} &= \begin{bmatrix} 0.245 & -0.784 & -0.0821 \\ 0.784 & 0.743 & -0.130 \\ 0.215 & -0.341 & -0.0492 \end{bmatrix} \Delta \mathbf{x}_k + \begin{bmatrix} -0.00158 \\ -0.00081 \\ 0.00191 \end{bmatrix} \Delta \mathbf{u}_k \\ \Delta \mathbf{y}_k &= \begin{bmatrix} 0 & 0 & 1 \end{bmatrix} \Delta \mathbf{x}_k \end{aligned} \quad (8)$$

E. Control Requirements

In order to design control systems, it is necessary to specify its requirements, since the control system design can vary depending on them. The requirements are often conflicting objectives. Among the wide variety of requirements for control systems, the following are some of the common ones:

- Stability (relative or total).
- Adaptable (robust).
- Minimum energy consumption.
- Optimal behavior.
- Time response properties (overshoot, growth time, etc.).
- Precision ($e_{ss} = 0$).

As it was stated, these requirements are often in conflict and they all cannot be satisfied completely, leading to a multi-objective optimization problem that tries to balance the requirements satisfied. This work will treat only with stability, precision and attempt to tweak time-response properties.

F. PID Controller

1) *Definition:* The PID controller is one of the most used schemes in industrial procedures, due to its easy tuning and usefulness in control systems in general [7]. As its name states, the PID controller was developed on the idea of taking the proportional, integral and derivative signal of the error. Recall that the error is the difference between the reference (desired state) and the current output of the system in study:

$$e(t) = r(t) - y(t) \quad (9)$$

The PID continuous controller has the following transfer function:

$$\frac{U(s)}{E(s)} = K_p \left[1 + \frac{1}{T_i s} + \frac{T_d s}{1 + N T_d s} \right] \quad (10)$$

where N is a relaxation constant, T_i is the integral time, T_d is the derivative time and K_p is the proportional gain; but in this work, the digital (discrete) PID controller will be used. Thus, the transfer function of said controller is given by

$$\frac{U(z)}{E(z)} = \frac{q_0 z^2 + q_1 z + q_2}{(z - r_1)(z - 1)}. \quad (11)$$

This controller has four adjustable parameters that depend on the original constants T_i , T_d , K_p and T (sample time). For more information on continuous and digital PID controllers, refer to [8].

2) *Tuning Methods:* The first and more simple tuning method is almost by brute force, changing the parameters accordingly to what is desired. In the literature, the effects on the time response of each parameter are well known; in Tab. I these effects are presented. The symbol + means that the parameter increases, - that it decreases and \approx that it does not show significant changes. The effects are shown for the growth time t_r , the maximum overshoot M_p , the settling time t_s and steady-state error e_{ss} .

The second tuning approximation is using the Zeigler-Nichols method. In this work, two variants of this method are applied: the reaction curve method and the sensitivity method.

Increment	Effect	t_r	M_p	t_s	e_{ss}
K_p	-	+	\approx	-	-
T_i	+	-	-	+	
T_d	\approx	-	-	-	\approx

Table I: Effects of the PID parameters in time response [8].

The reaction curve method [8] is based on the step response of the system. This method requires a stable plant; Fig. 3 illustrates how to obtain the parameters R (slope) and L (delay) from the tangent line at the inflection point.

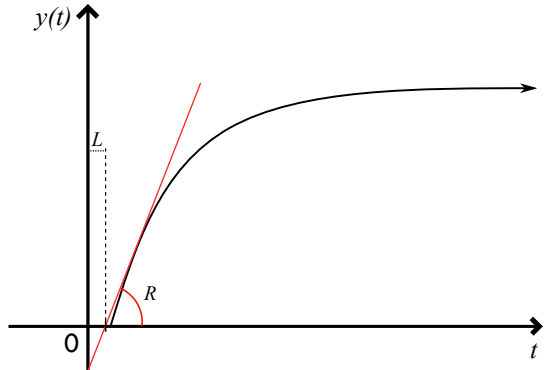


Figure 3: Reaction curve method.

Based on the values for R and L , the PID parameters can be calculated as follows:

$$\begin{aligned} K_p &= \frac{1.2}{RL} \\ T_i &= 2L \\ T_d &= 0.5L \end{aligned} \quad (12)$$

Although, there are many approaches to this tuning; in this work, the Chien-Hrones-Reswick rules for parameters will also be tested; the expressions to calculate the parameters are presented in Tab. II. Note that the percentages refer to the maximum overshoot of the time response.

0%	20%
$K_p = 0.95RL$	$K_p = \frac{1.2}{RL}$
$T_i = 2.4L$	$T_i = 2L$
$T_d = 0.42L$	$T_d = 0.42L$

Table II: Chien-Hrones-Reswick rules for tuning.

Remark: for discrete systems $L = L + T/2$. The regulability (level of difficulty) of the system can be calculated: $S_0 = RL$; if this value is near zero, it means that the system has a good regulability, but for values greater than 0.8 it does not [8].

On the other hand, the sensitivity method [8] is based on the critically-stable time response, where the gain and the period of this response is used to calculate the parameters; this can

be also calculated using the Bode diagram, through the gain margin and its respective frequency as follows:

$$\begin{aligned} K_u &= 10^{\frac{M_G}{20}} \\ T_u &= \frac{2\pi}{\omega_{cf}} \end{aligned} \quad (13)$$

and then calculate the PID parameters using

$$\begin{aligned} K_p &= 0.6K_u \\ T_i &= \frac{T_u}{2} \\ T_d &= \frac{T_u}{8} \end{aligned} \quad (14)$$

Finally, one last analytical tuning method will be presented. Suppose you have a discrete transfer function $G(z)$ and let the discrete PID controller transfer function be $H(z)$, the closed-loop transfer function for the controlled system is

$$G_{cl}(z) = \frac{H(z)G(z)}{1 + H(z)G(z)} \quad (15)$$

Therefore, the denominator of the equivalent transfer function is $P(z) = \text{Num}\{1 + G(z)H(z)\}$; note that $P(z)$ is polynomial in terms of the discrete PID parameters q_0, q_1, q_2 and r_1 .

The main idea of this method is to find these PID parameters based on assigning poles to desired values and solving the system of equations for these parameters.

G. Controllability Analysis

A system is said to be controllable if there exist an unconstrained control vector that can transfer the system from an initial state $x(t_0)$ to any other state in a finite interval of time [7, p. 675]. In order to check for controllability of a linear system, the following condition must be satisfied:

$$\text{rank}(M_c) = n \quad (16)$$

where M_c is the controllability matrix and n is the order of the system. The controllability matrix is constructed as follows:

$$M_c = [\mathbf{B} \quad \mathbf{AB} \quad \dots \quad \mathbf{A}^{n-1}\mathbf{B}] \quad (17)$$

For proofs of this condition and additional information, refer to [7, pp. 675-682].

H. Discrete Linear Feedback Controller: Pole Assignment

The idea with this controller is, using the information of all the states of a controllable system, stabilizing the output in 0 when the input reference has that same value by assigning poles. This controller is really powerful as uses more information of the system, instead of only the output as the PID controller does; on the other hand, it can only be applied in real systems when all of the states can be measured which is not always easily done.

For a SISO linear system, if n is the number of states of the system, it is done by finding a vector $\mathbf{K}_{(1 \times n)}$ such that the input of the system is given by:

$$u(k) = -\mathbf{K}x(k) \quad (18)$$

In this manner, it can be found that the closed-loop system has the form of:

$$\begin{aligned} \mathbf{x}(k+1) &= \Phi\mathbf{x}(k) + \Gamma\mathbf{u}(k) \\ &\downarrow \\ \mathbf{x}(k+1) &= (\Phi - \Gamma\mathbf{K})\mathbf{x}(k) \end{aligned} \quad (19)$$

So, the poles of this closed-loop system are given by the eigenvalues of the matrix $(\Phi - \Gamma\mathbf{K})$; therefore, the idea would be to find this vector that makes the matrix have some desired poles. For a SISO system, the classical method to find this vector is the Ackerman method [9] which is going to be used in this paper. The block model is shown in 4.

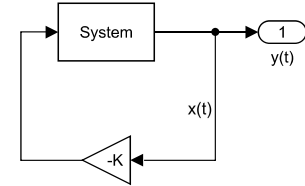


Figure 4: Block model for a feedback controller with a reference of 0.

In MATLAB, to use the ackerman method the function is `acker` which uses the following syntax: $\mathbf{K} = \text{acker}(\Phi, \Gamma, \text{poles})$ where `poles` are the desired poles for the system. On the other hand, the function `place`, following the same syntax, also finds this vector with a different method but, with the restriction that the multiplicity of each pole can not be larger than the number of inputs of the system. The advantage of the second method is that it can be used when the system has different inputs.

I. Discrete Linear Feedback Controller: Pole Assignment without e_{ss}

This controller has the same purpose as the one explained above, with the difference that the input reference is not necessarily 0. In this manner, to reduce completely the e_{ss} it is important to add an integrator to the plant. With this addition, the following system is obtained (for a SISO system):

$$\begin{aligned} \begin{bmatrix} \mathbf{x}(k+1) \\ \mathbf{v}(k+1) \end{bmatrix} &= \begin{bmatrix} \Phi & \mathbf{0}_{n \times 1} \\ -\mathbf{C} & 1 \end{bmatrix} \begin{bmatrix} \mathbf{x}(k) \\ \mathbf{v}(k) \end{bmatrix} + \begin{bmatrix} \Gamma \\ 0 \end{bmatrix} \mathbf{u}(k) + \begin{bmatrix} \mathbf{0} \\ 1 \end{bmatrix} \mathbf{r}(k) \\ &\downarrow \\ \tilde{\mathbf{x}}(k+1) &= \tilde{\Phi}\tilde{\mathbf{x}}(k) + \tilde{\Gamma}_1\mathbf{u}(k) + \tilde{\Gamma}_2\mathbf{r}(k) \end{aligned} \quad (20)$$

Then, the idea is to find a vector $\tilde{\mathbf{K}}$ such that the matrix $(\tilde{\Phi} - \tilde{\Gamma}_1\tilde{\mathbf{K}})$ has some desired poles. In this manner, using the methods explained above, we obtain the following:

$$\tilde{\mathbf{K}} = [\mathbf{K} \quad \mathbf{L}] \quad (21)$$

The block model for this controller is shown in 5.

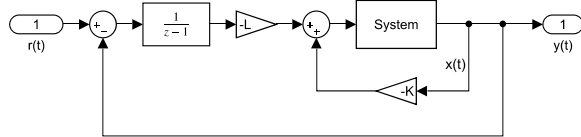


Figure 5: Block model for a feedback controller with an additional integrator.

J. Uncertainty Analysis

Although there is a wide variety of uncertainty and sensitivity analysis methods, this work uses only an empirical approach to the formal uncertainty analysis. The main objective of the method here presented is to find ranges of the parameter R_a where the controller behaves properly (no steady-state error and stability) for each of the controllers obtained. The idea is to change upwards and downwards R_a by a 10% of its initial value; based on this results, the changes can be extended in order to find ranges where the controller works or, at least, it does not saturate.

III. RESULTS

Remark: all the time-responses of the nonlinear Rössler system are presented subtracting the operation point, in order to see the references and stabilization easily.

A. Discrete PID Controller

1) *Tuning by Reaction Curve:* As described in section II-F2, the tuning of a PID controller can be performed through the reaction curve. For obtaining the reaction curve, the linearized Rössler system (equation 7) was simulated for 50s using 4th-order Runge-Kutta method with time step of 0.01s, with input of $\Delta u = 2V$. The reaction curve obtained is presented in Fig. 6.

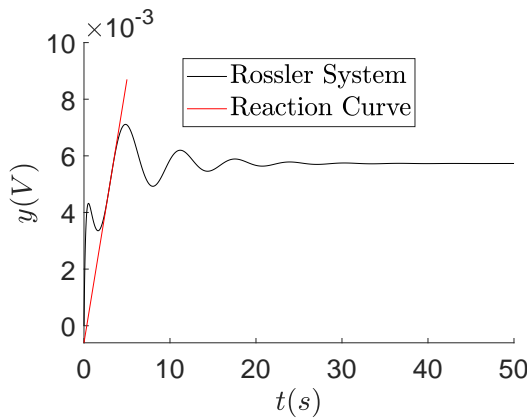


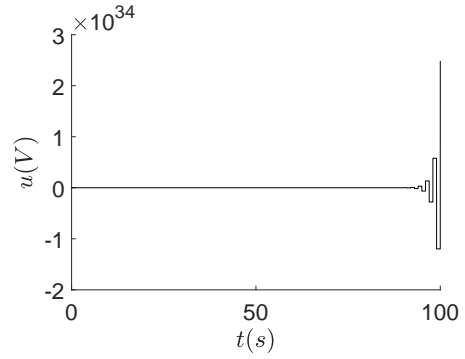
Figure 6: Reaction curve.

Calculating the slope of this line and the delay: $R = 0.0019$ and $L = 0.8239$. This values yield the following PID parameters:

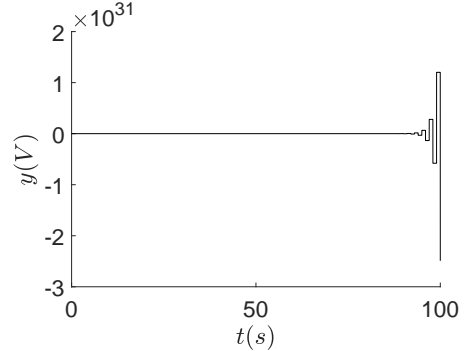
$$K_p = 782.8568$$

$$T_i = 1.6478$$

$$T_d = 0.4119$$



(a) Control action.



(b) Output.

Figure 7: Linear system simulation with discrete Zeigler-Nichols controller.

Applying the formulas for the discrete PID, yields

$$q_0 = 1342.9$$

$$q_1 = -1190.3$$

$$q_2 = 322.4894$$

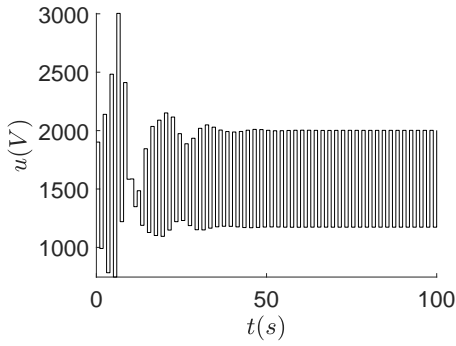
Therefore, the transfer function of the discrete PID controller is

$$\frac{U(z)}{E(z)} = \frac{1342.9z^2 - 1190.3z + 322.4894}{z(z-1)} \quad (22)$$

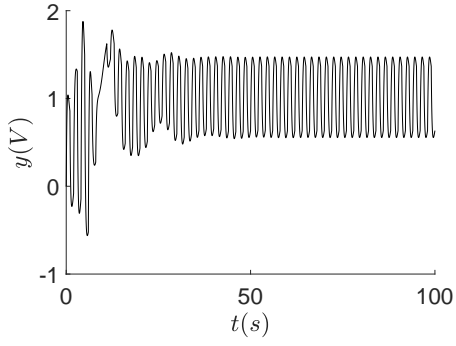
Now, a simulation applying this controller was performed using as reference $r(t) = 1V$, for both the linear and nonlinear systems. In Fig. 7, the control action and the output of the linear system is presented; note that this PID controller makes the linear system unstable, which is not desired.

On the other hand, the control action and the output of the nonlinear system is shown in Fig. 8. It is important to highlight that a saturation was selected for the input, i.e. a minimum and maximum value for the control action was added. This saturation was selected from 0V to a maximum of 1500V, since it is a reasonable interval from a power source as input; note that the control action shown in Fig. 8 a. was extracted before the saturation.

Moreover, the tuning was performed with the reaction curve but applying the Chien-Hrones-Reswick rules for 0%



(a) Control action.



(b) Output.

Figure 8: Rössler system simulation with discrete Zeigler-Nichols controller.

of maximum overshoot. The discrete PID controller is

$$\frac{U(z)}{E(z)} = \frac{990.9356z^2 - 891.9540z + 214.4554}{z(z-1)}$$

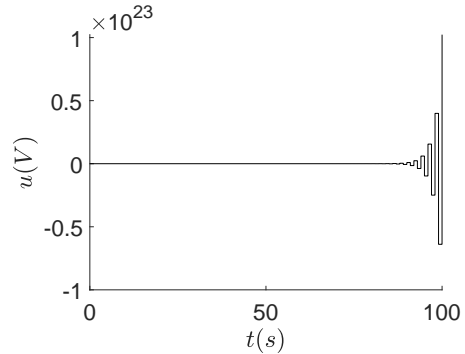
And the same simulation was performed with $r(t) = 1V$. The plots presented in Fig. 9 show the control action for the linear system applying the Chien-Hrones-Reswick controller. Note that, just as Zeigler-Nichols controller, it makes the linear system unstable.

Finally, the control action and system output of the Rössler nonlinear equations in study are presented in Fig. 10. Again, there is saturation in the control action

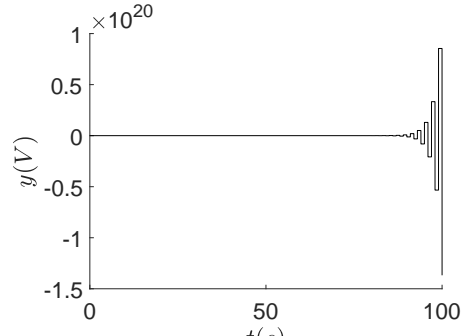
2) Tuning by Sensitivity Curve: The second method presented in II-F2 is through the gain margin M_G and its frequency ω_{cf} . In previous work [10], the respective gain margin and frequency was obtained: $M_G = 52.7993dB$ and $\omega_{cf} = 3.1416rad/s$, which yield $K_u = 436.48$ and $T_u = 2s$. Therefore, the discrete PID controller with the sensitivity method is

$$\frac{U(z)}{E(z)} = \frac{458.3046z^2 - 261.8883z + 65.4721}{z(z-1)}$$

In order to make a comparison with the previously obtained PID controllers, the same simulation will be performed with $r(t) = 1$. In Fig. 11, the control action and output for the nonlinear Rössler system is presented. Note that, unlike the previous PID controllers, this one does not unstabilize the



(a) Control action.



(b) Output.

Figure 9: Linear system simulation with discrete Chien-Hrones-Reswick controller.

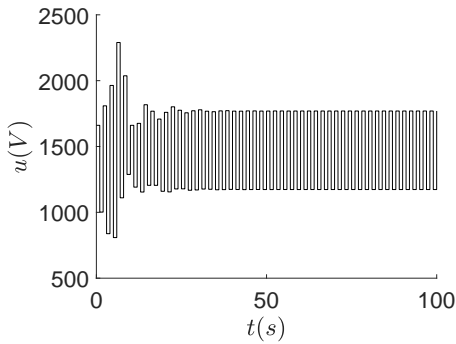
system and can eliminate steady-state error for this particular reference.

It is important to highlight that the linear system is not presented since it works perfectly with this controller. Note that the system shows stabilization in 1V. Now that a functional controller was found, we proceed to make an analysis on this controller.

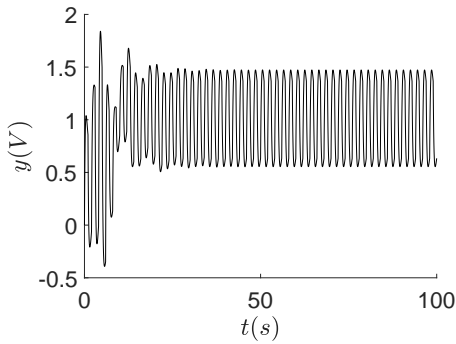
In order to start the analysis, the following plots (Fig. 12) show the steady-state values for the output and the control signal for different inputs; this figure was constructed following the same ideas behind a linearity curve (see [10]). Note that the plots show that the nonlinear system diverges from the linear controlled system, due to the saturation defined in the system.

Now, it was desired test the controller with time-dependent references. The first simulation was for a reference $r(t) = 0.01t$ with $t \in [0, 100]$. The result of this simulation for both control and output is presented in Fig. 13; note that the control system makes a good attempt to stabilize the system exactly at the reference, making the error almost constant. Note that the control action remains inside the saturation interval, meaning that the control does not exceed the predefined limit.

Another simulation was executed but for a slightly larger slope: $r(t) = 0.018$. The results of this simulation are displayed in Fig. 14. Note that the control action reaches its maximum value near 90s, therefore there is saturation and the

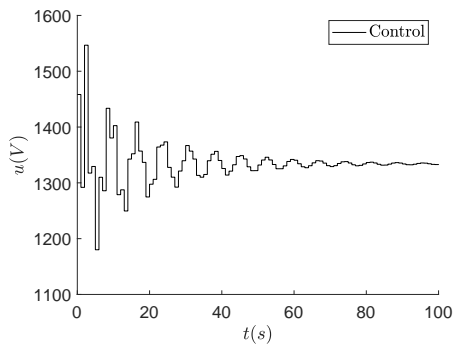


(a) Control action.

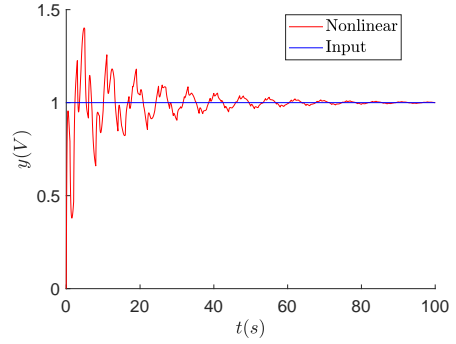


(b) Output.

Figure 10: Rössler system simulation with discrete Chien-Hrones-Reswick controller.

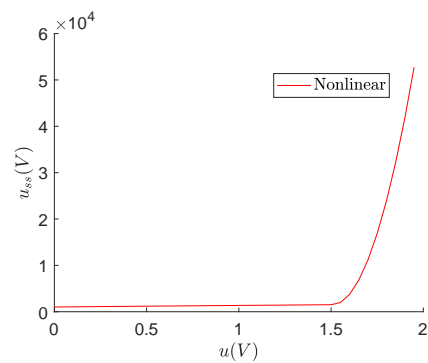


(a) Control action.

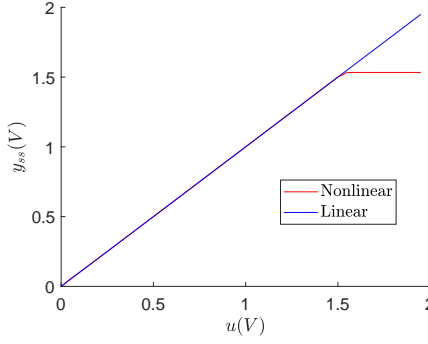


(b) Output.

Figure 11: Rössler system simulation with discrete sensitivity controller.

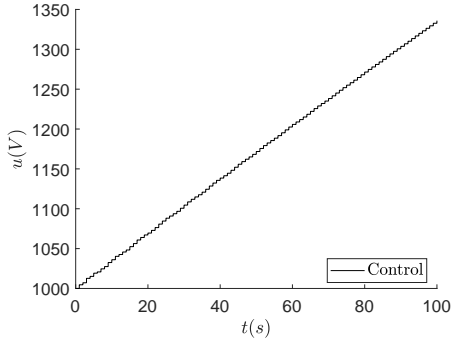


(a) Control action.

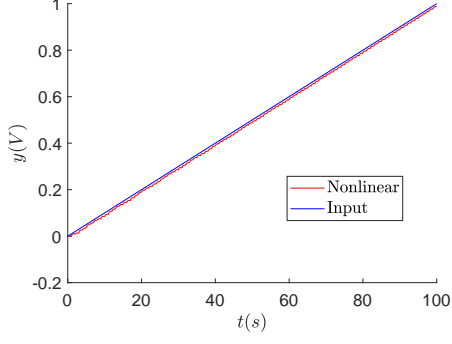


(b) Output.

Figure 12: Sensitivity linear vs. nonlinear system.

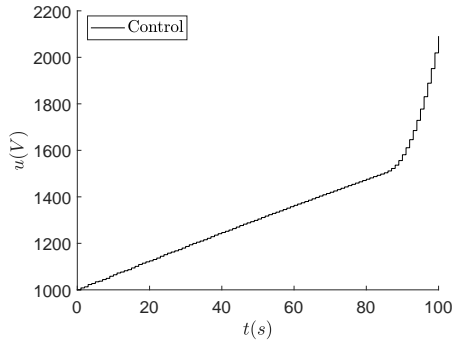


(a) Control action.

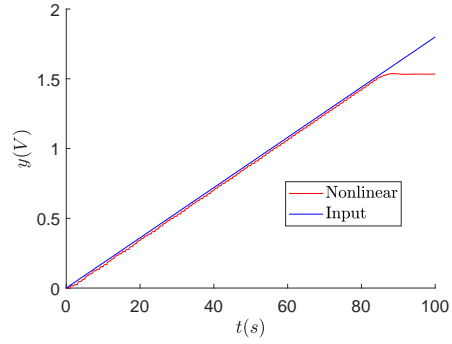


(b) Output.

Figure 13: Rössler system simulation with discrete sensitivity controller for $r(t) = 0.01t$.



(a) Control action.



(b) Output.

Figure 14: Rössler system simulation with discrete sensitivity controller for $r(t) = 0.018t$.

nonlinear system can no longer “follow” the reference, as the output shows: around 90s both curves diverge.

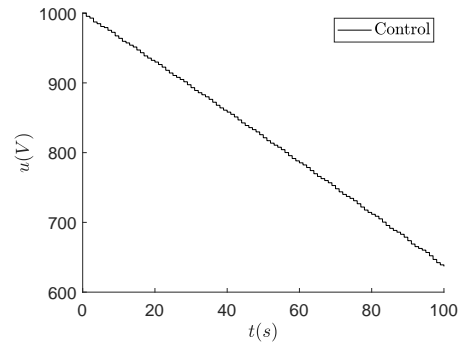
As it will be discussed later on the Analysis section IV, this discrete PID controller has an upper bound. In order to find a lower bound, negative slope references will be analyzed. For a reference of $r(t) = -0.01$, Fig. 15 shows the control and output; just as its positive counterpart, the nonlinear “follows” the negative reference with almost a constant error.

For a slightly more negative slope ($r(t) = -0.03t$), the plots presented in Fig. 16 show that the control action needed is negative, which is a contradiction to the minimum control action set, making the nonlinear system diverge from the reference.

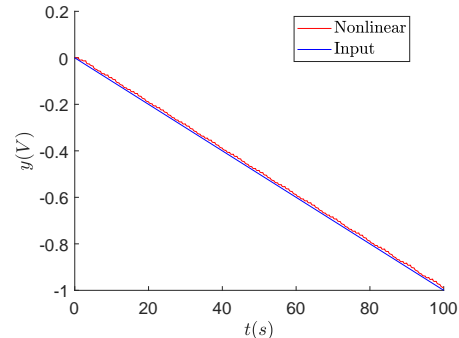
For a better visualization of the effect of this lower saturation, one last simulation was performed with the discrete sensitivity PID controller with $r(t) = -0.05t$; Fig. 17 shows the results. Note that the control action is negative from around 50s, at that exact time the nonlinear Rössler system diverges completely from the reference and starts to behave chaotically.

Finally, a lower bound for the reference was found by iterative simulation: $r(t) = -0.25$; Fig. 18 shows the control action and output with the sensitivity discrete PID controller on its critically stable state.

3) Tuning by Analytic Procedure: In previous work [10], a second order approximation for the linearized Rössler system

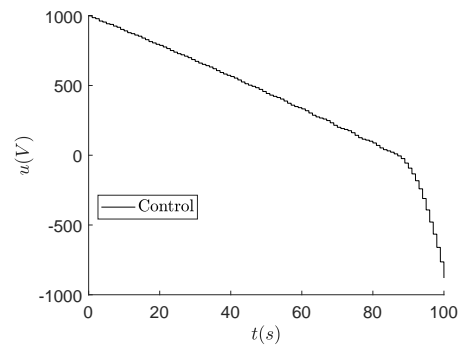


(a) Control action.

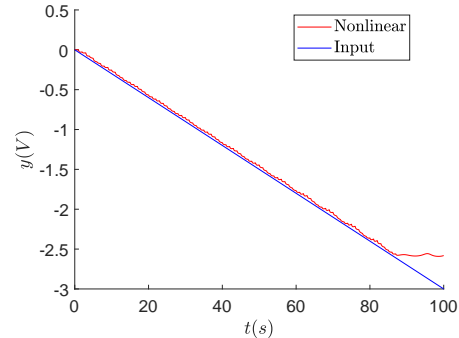


(b) Output.

Figure 15: Rössler system simulation with discrete sensitivity controller for $r(t) = -0.01t$.

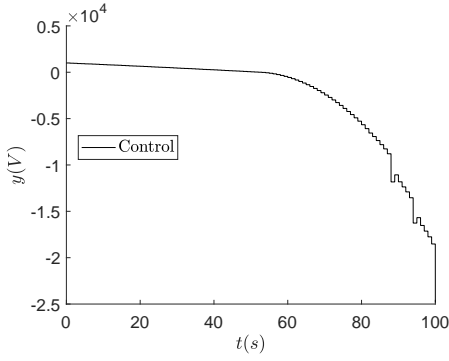


(a) Control action.

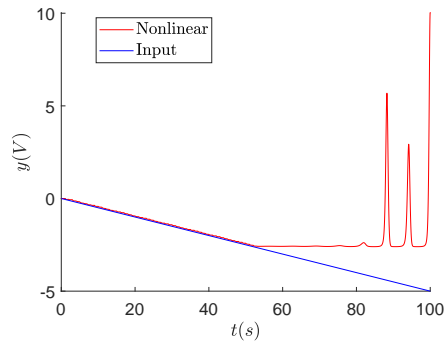


(b) Output.

Figure 16: Rössler system simulation with discrete sensitivity controller for $r(t) = -0.03t$.

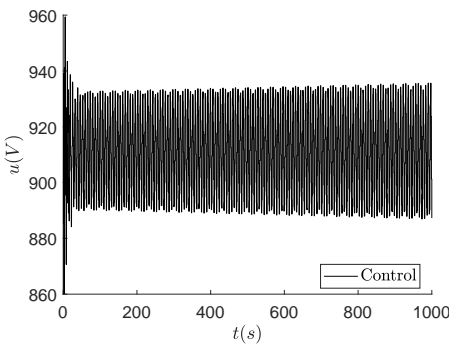


(a) Control action.

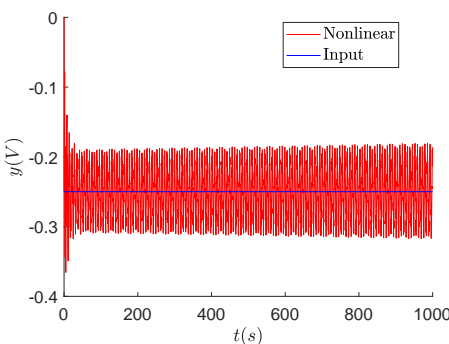


(b) Output.

Figure 17: Rössler system simulation with discrete sensitivity controller for $r(t) = -0.05t$.

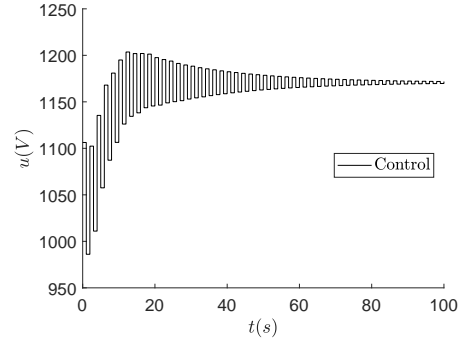


(a) Control action.

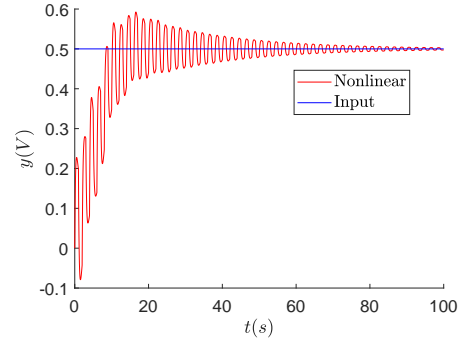


(b) Output.

Figure 18: Rössler system simulation with discrete sensitivity controller for $r(t) = -0.25t$.



(a) Control action.



(b) Output.

Figure 19: Rössler system simulation with discrete analytic controller for $r(t) = 0.5$.

was found and has the following transfer function:

$$\tilde{G}(s) = \frac{0.001461}{s^2 + 0.5887s + 0.5102} \quad (23)$$

and applying a discretization of this transfer function with sample time of $T = 1s$, the following discrete system was obtained:

$$\tilde{G}(z) = \frac{0.000582z + 0.0004769}{z^2 - 1.185z + 0.5547} \quad (24)$$

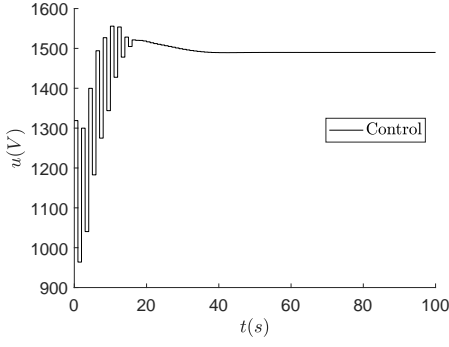
The analytic procedure was applied setting all four poles in 0.5 (closed-loop system), which yields the following discrete PID controller

$$\frac{U(z)}{E(z)} = \frac{212.6018z^2 - 355.9319z + 202.3534}{(z + 0.0613)(z - 1)} \quad (25)$$

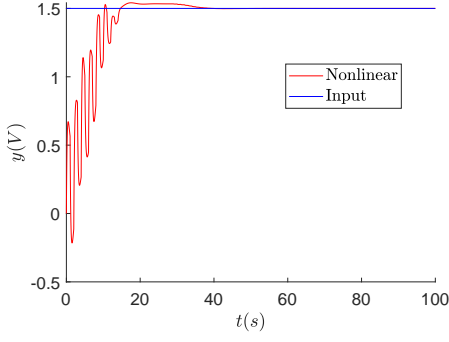
With the obtained discrete PID controller, a simulation was performed for a reference of $r(t) = 0.5$ (Fig. 19), note that the output is fast and it does not have steady-state error but the response shows high frequency oscillations.

Next, a simulation for $r(t) = 1.5$ was performed and presented in Fig. 20. Notice the high frequency oscillation in transitory state but the smooth stabilization exactly at 1.5, eliminating the steady-state error.

Finally, another simulation was executed for a negative reference value of $r(t) = -1.2$. The control action and the system output are shown in Fig. 21. This time response is quite fast and shows high frequency oscillation as well. The system does not present steady-state error.

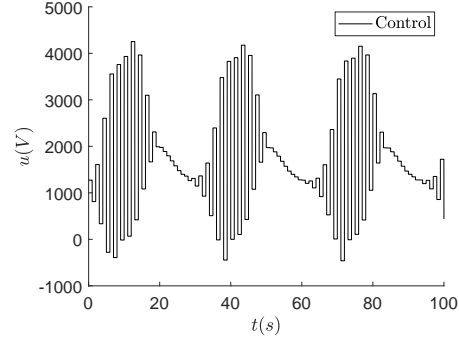


(a) Control action.

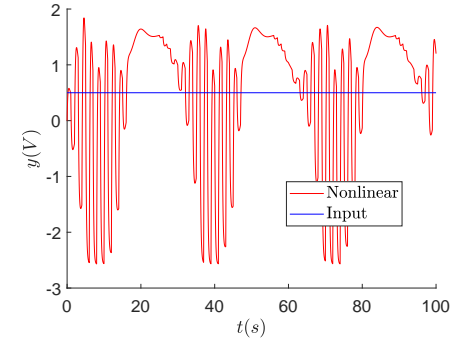


(b) Output.

Figure 20: Rössler system simulation with discrete analytic controller for $r(t) = 1.5$.



(a) Control action.



(b) Output.

Figure 22: Rössler system simulation with discrete analytic controller for $r(t) = 0.5$ with poles in 0.4.

Moreover, it was attempted to take the poles to $z = 0.4$, which yields the following PID controller

$$\frac{U(z)}{E(z)} = \frac{547.6520z^2 - 788.6674z + 363.4062}{(z + 0.2663)(z - 1)} \quad (26)$$

In order to test this controller, a reference of $r(t) = 0.5$ was used for the simulation presented in Fig. 22; this simulation shows that the PID controller fails and does not behave properly.

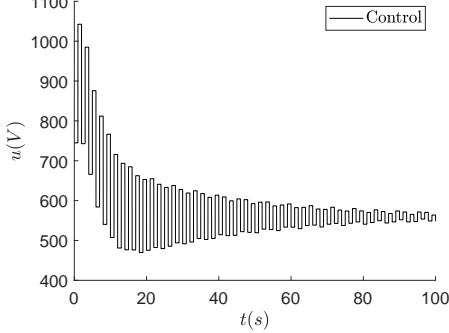
B. Discrete State Feedback Controller: Pole Assignment

It was desired to set the poles exactly at the origin, in $z = 0$ (dead-beat controller), with the state feedback control scheme. Applying the method described in II-H, the obtained gain vector is

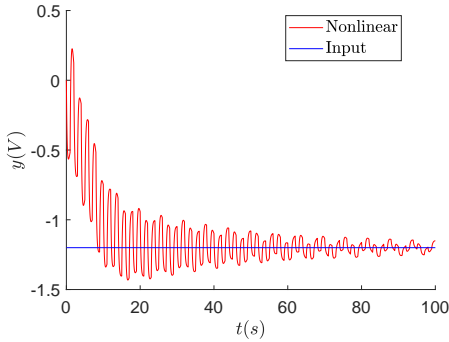
$$K = [-438.5251, -103.1074, 86.1249] \quad (27)$$

In order to test the obtained controller, some simulations were performed. Keep in mind that this method is only for $r(t) = 0$, therefore the simulations are performed changing the initial conditions for the state x_3 (output). The first change is in $0.1V$ and the obtained results are presented in Fig. 23.

Next, a simulation changing 50 in the initial conditions of x_3 was carried out; in Fig. 24 the control action and the system output can be appreciated. Note that the system can eliminate steady-state error but at the very beginning there is saturation.

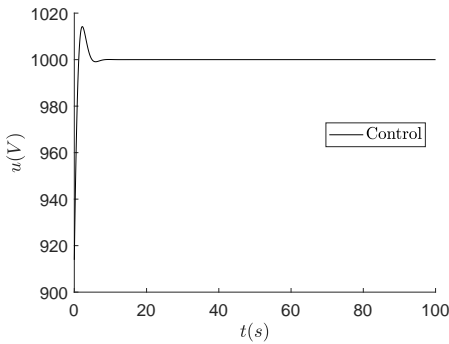


(a) Control action.

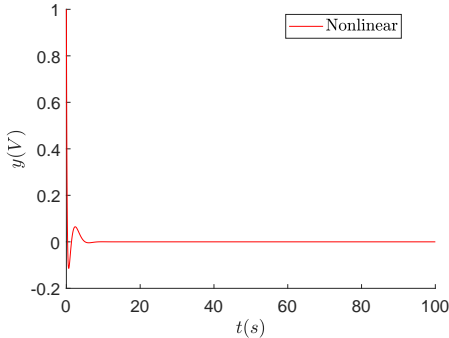


(b) Output.

Figure 21: Rössler system simulation with discrete analytic controller for $r(t) = -1.2$.

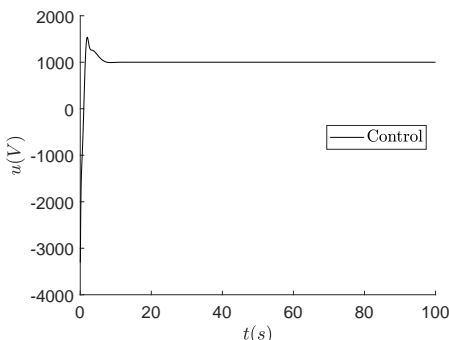


(a) Control action.

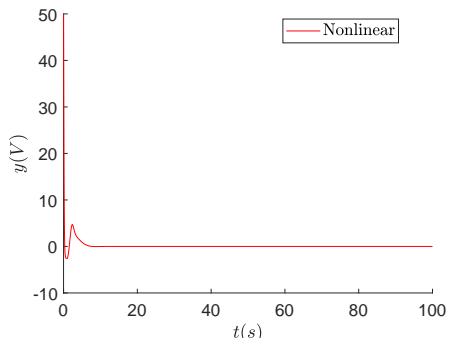


(b) Output.

Figure 23: Rössler system simulation with discrete state feedback controller with 0.1 in x_3 .

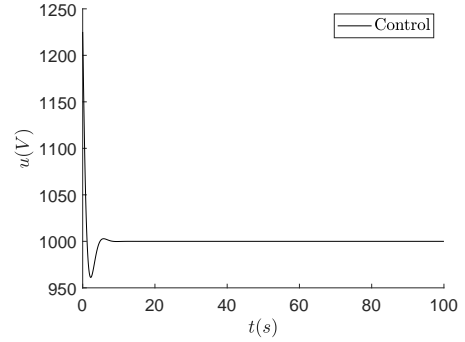


(a) Control action.

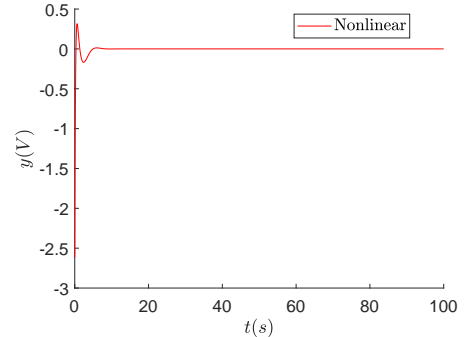


(b) Output.

Figure 24: Rössler system simulation with discrete state feedback controller with 50 in x_3 .



(a) Control action.



(b) Output.

Figure 25: Rössler system simulation with discrete state feedback controller with -2.6 in x_3 .

Now, testing for a negative change in the initial condition, it was subtracted 2.6 from the initial conditions of x_3 . In Fig. 25 these results are presented for the control and the output. Note that there is no saturation neither steady-state error.

C. Discrete State Feedback Controller: Pole Assignment without e_{ss}

In this section, all the desired poles for the system were $z = 0.5$ (prior analysis yielded that $z = 0$ required way too much energy). Carrying out the procedures depicted in section II-I, the gain vectors are

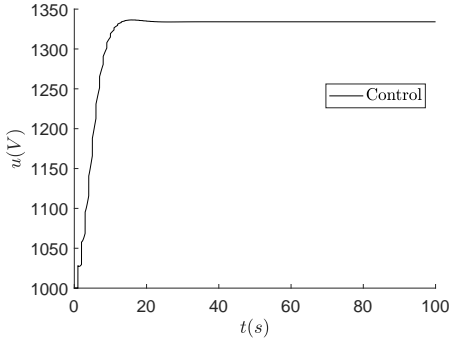
$$K = [-24.9703, 156.6863, 14.2350] \quad (28)$$

$$L = -28.1628$$

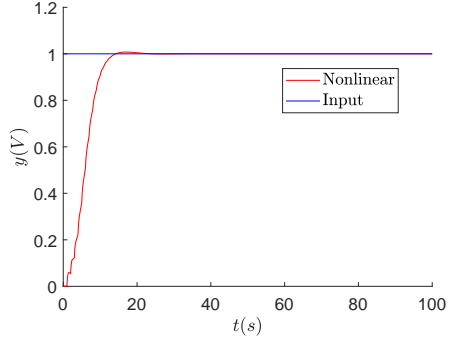
It has been mentioned that this controller allows for $r(t) \neq 0$; therefore, in order to test this controller and to compare with the previously obtained ones, a simulation was conducted using $r(t) = 1$. The results for said simulation are shown in Fig. 26. Note that this controller achieves stability and can eliminate steady-state error for $r(t) = 1$.

Another simulation was performed using $r(t) = 1.5$ (Fig. 27) and the system showed proper behavior with this controller, eliminating steady-state error but with slightly larger overshoot without saturation.

Finally, one last constant reference was simulated: $r(t) = -2$. As shown in Fig. 28, the controller manages to stabilize the system eliminating steady-state error but with high frequency oscillations.

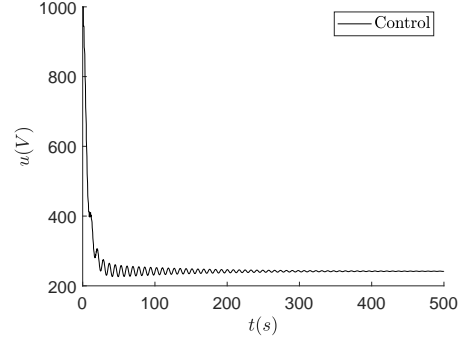


(a) Control action.

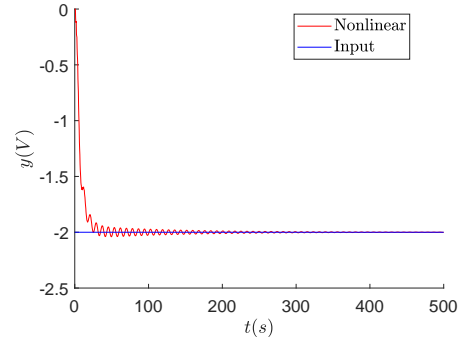


(b) Output.

Figure 26: Rössler system simulation with discrete state feedback controller $r(t) = 1$.

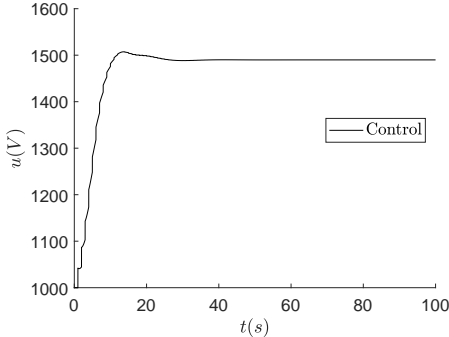


(a) Control action.

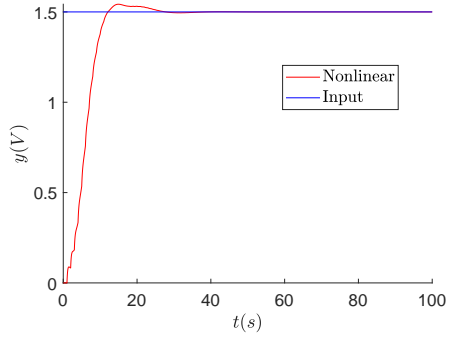


(b) Output.

Figure 28: Rössler system simulation with discrete state feedback controller $r(t) = -2$.



(a) Control action.



(b) Output.

Figure 27: Rössler system simulation with discrete state feedback controller $r(t) = 1.5$.

Next, a variable reference was tested, using $r(t) = 0.01t$. The control action and the system's output is presented in 29; notice that the steady-state for the Rössler system is parallel to the desired reference, this will be discussed in the next section.

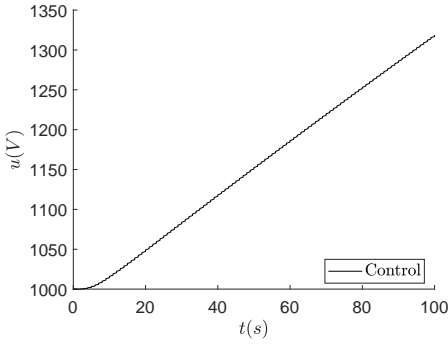
D. Uncertainty Analysis

The uncertainty analysis was performed for the analytic discrete PID controller, for the state feedback controller with and without steady-state error. Applying the procedure described in section II-J, the parameter $R_a = 500k\Omega$ will be first changed by 10% (upwards and downwards) and then some other important values will be selected. The following simulations are set for $r(t) = 1$.

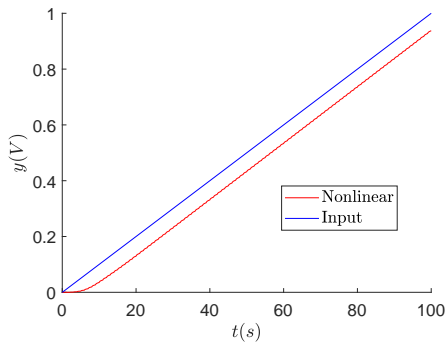
For the analytic discrete PID controller, the first two simulations are for changing R_a by 10% upwards ($550k\Omega$) and downwards ($450k\Omega$). In Figs. 30-31, these simulations are presented, notice that this controller works properly for these changes in R_a .

Next, a larger change upwards in R_a was performed: $R_a = 2500k\Omega$. In Fig. 32 the results for the controller and the output are presented, note that the system achieves stability and steady-state error elimination with smaller overshoot than the previous simulations; but the control action is on the limit, as it is about to reach its maximum value.

Finally, a larger change downwards was performed $R_a = 300k\Omega$. Fig. 33 shows the results for this simulation. Notice that the system is critically stable around $y(t) = 1V$, this

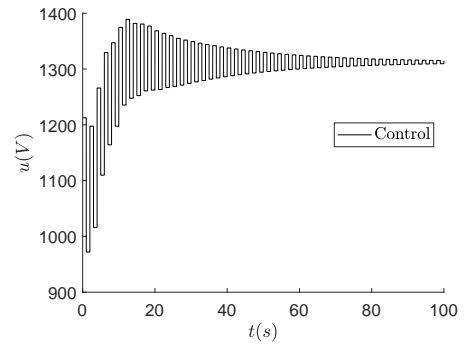


(a) Control action.

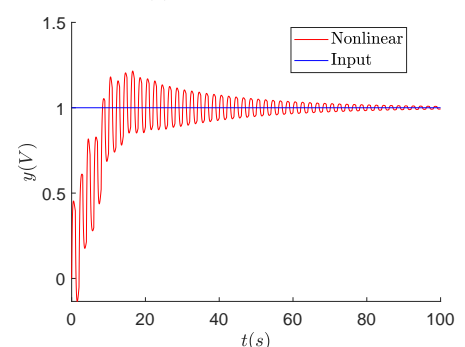


(b) Output.

Figure 29: Rössler system simulation with discrete state feedback controller $r(t) = -2$.

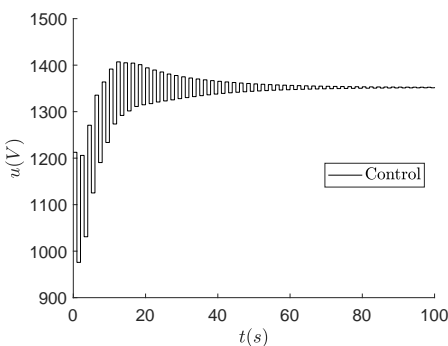


(a) Control action.

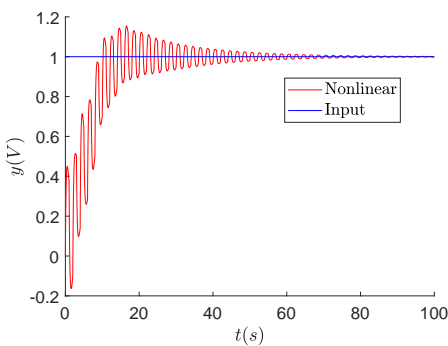


(b) Output.

Figure 31: Analytic discrete PID controller for $R_a = 450k\Omega$.

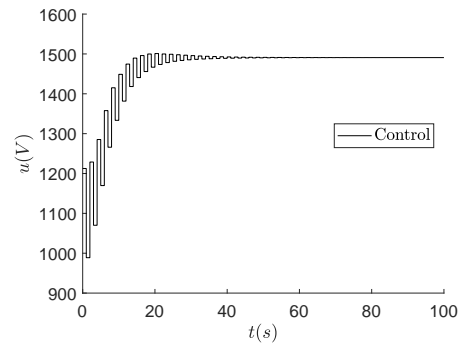


(a) Control action.

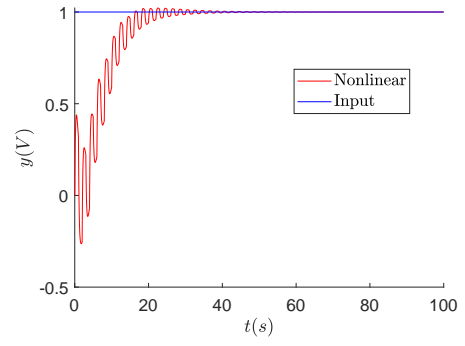


(b) Output.

Figure 30: Analytic discrete PID controller for $R_a = 550k\Omega$.

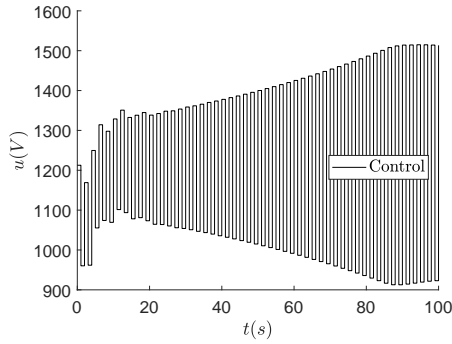


(a) Control action.

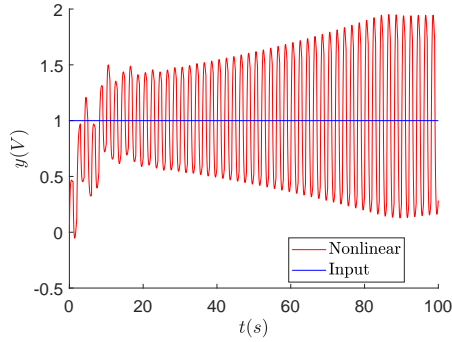


(b) Output.

Figure 32: Analytic discrete PID controller for $R_a = 2500k\Omega$.



(a) Control action.



(b) Output.

Figure 33: Analytic discrete PID controller for $R_a = 300k\Omega$.

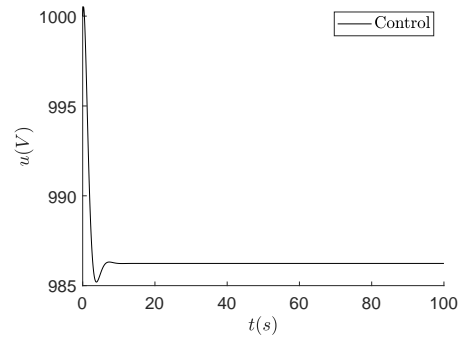
implies that the controller is on the edge of making the system unstable and it cannot eliminate steady-state error. Note that the control signal is almost saturated.

For the discrete state feedback controller, the same procedure was attempted. The parameter R_a was changed to $550k\Omega$ and $450k\Omega$. Figs. 34-35 show both simulations (recall that $r(t) = 0$ in these controllers), where it can be observed that these controller does not work properly (they do not stabilize in the reference).

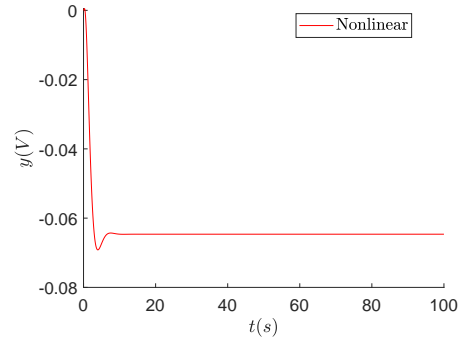
Finally, the discrete state feedback controller with no steady-state error was analyzed with the same parameters as the discrete analytical PID controller. Thus, the first two simulations are for $R_a = 550k\Omega$ and $R_a = 450k\Omega$, displayed in Figs. 36-37, as it can be seen, the controller works properly for both changes, showing no steady-state error and good behavior (no significant overshoot or oscillation).

Now, the same simulation was executed for $R_a = 3000k\omega$ and the control signal and output can be observed in Fig. 38. Notice that the control signal is almost saturated but the controller works perfectly, without overshoot relatively fast stabilization.

Lastly, the parameter R_a was set to $250k\Omega$ and the simulation was conducted one last time. These results are presented in Fig. 39; this simulation show that the controller cannot work properly, since the system reaches a critically-stable state, showing undesired steady-state error (although the control signal is not saturated).

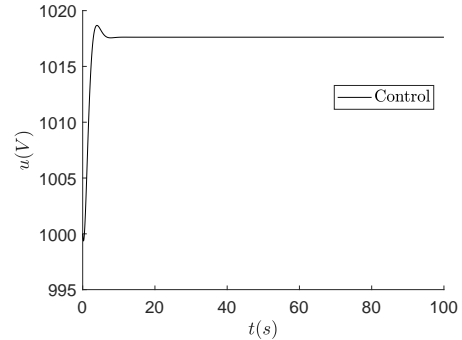


(a) Control action.

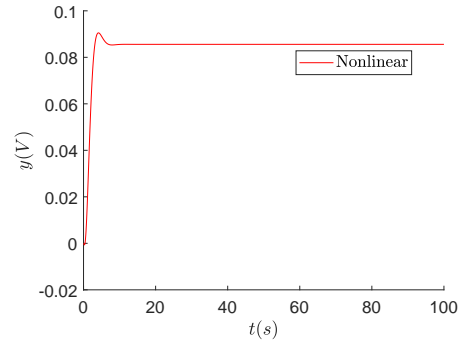


(b) Output.

Figure 34: Discrete state feedback controller controller for $R_a = 550k\Omega$.

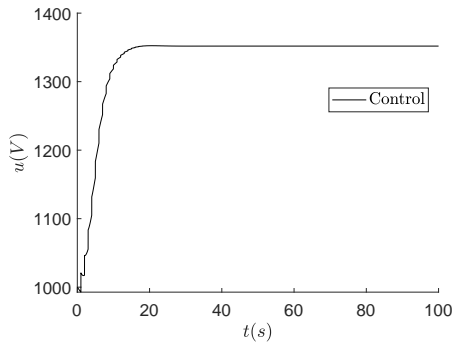


(a) Control action.

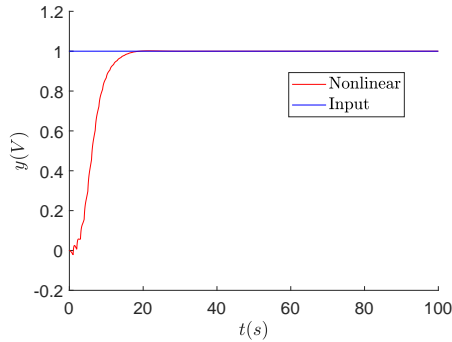


(b) Output.

Figure 35: Discrete state feedback controller controller for $R_a = 450k\Omega$.

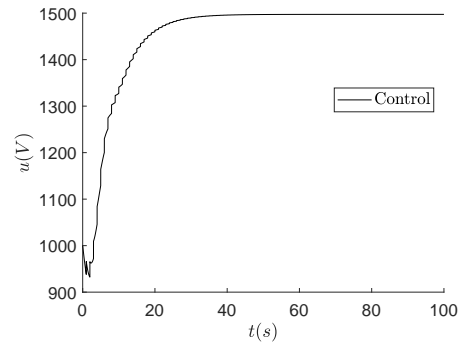


(a) Control action.

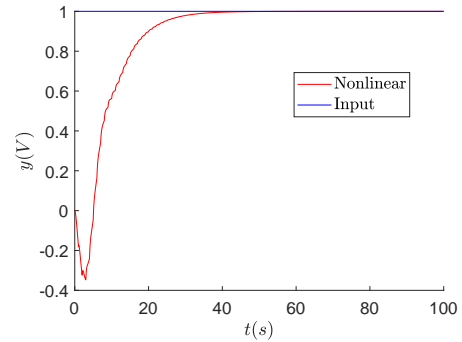


(b) Output.

Figure 36: Discrete state feedback controller ($r(t) \neq 0$) controller for $R_a = 550k\Omega$.

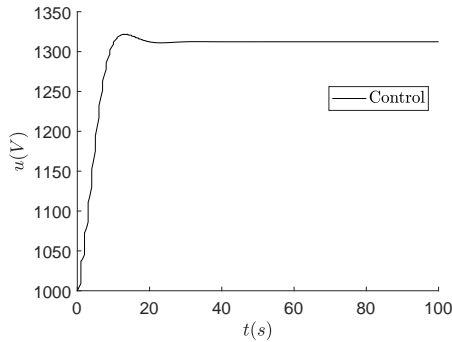


(a) Control action.

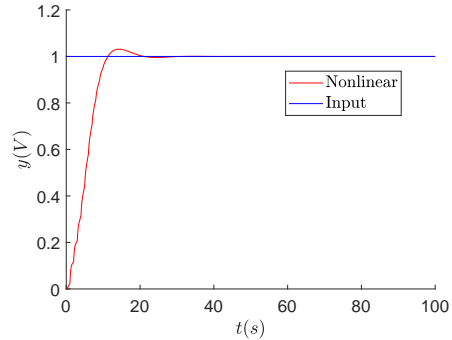


(b) Output.

Figure 38: Discrete state feedback controller ($r(t) \neq 0$) controller for $R_a = 3000k\Omega$.

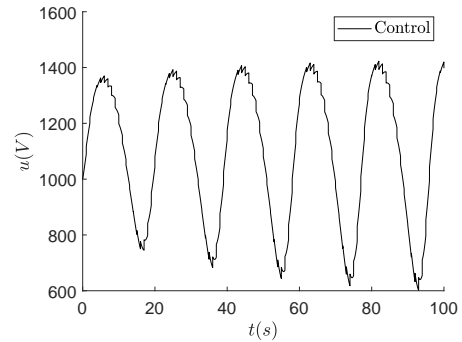


(a) Control action.

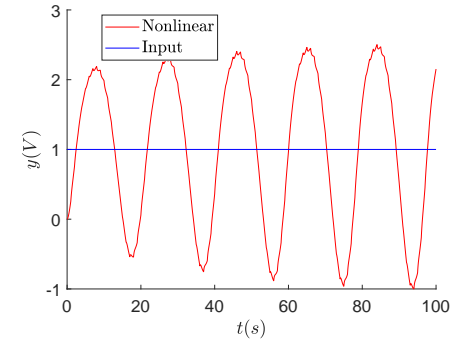


(b) Output.

Figure 37: Discrete state feedback controller ($r(t) \neq 0$) controller for $R_a = 450k\Omega$.



(a) Control action.



(b) Output.

Figure 39: Discrete state feedback controller ($r(t) \neq 0$) controller for $R_a = 250k\Omega$.

IV. RESULTS ANALYSIS

A. Discrete PID Controller

1) *Reaction curve method:* This method did not work neither using the Ziegler-Nichols nor the Chien-Hrones-Reswick rules as seen in Figs. 7-10. Although the value for RL , in both cases, is within the zone where the system is highly controllable there is an underlying problem within: the proportional gain gets larger as the value for the RL becomes smaller. In this manner, in [10] it was found that the maximum gain for the closed-loop Rössler system was $k_{max} = 601.2835$ for preserving stability and, the proportional gains for each of the methods provides a higher value. Furthermore, the Rössler system is a non-minimum phase attractor so when obtaining the line that crosses the inflection point it is affected by this property. Lastly, even if the problems explained above did not affect this controller, the parameters for the PID controller are large enough to always saturate the system.

Therefore, this heuristic fails as the proportional constant is higher than the one that the system can manage, the inflection point is not easily found with a non-minimum phase system and it does a large control action saturating the system.

2) *Sensitivity method:* As it is seen in Fig. 11, this controller completely reduces the e_{ss} with an input of 1. This, different from the last PID, has a much better result as it takes into account the maximum gain obtained in the discrete system, assuring that the controller does not have undesired properties. Now, in Fig. 12 it is seen how this controller acts perfectly on the linear system, as it should, while the Rössler system it stops working around the $u = 1.6$; this is an expected behaviour, as the linear system is only a representation of the original one and, at the same time, the real system has a saturation which does not allow for unrealistically large inputs. On the other hand, around $u = -0.25$ it is found the lower bound for this reference (Fig. 18, as it is critically stable and smaller values will unstabilize the system).

Furthermore, this controller also works for ramp inputs, although in a smaller interval for values of the slope. As seen in Figs. 13 and 15, this controller effectively controls the system to have exactly the input given; although it does not match perfectly the input, this occurs because the PID controller is discrete therefore it can only act upon the system every time sample. It is important to notice, that if the system would be simulated more time this controller would not work as the input would surpass the maximum value found before; in this manner, the interval maximum and minimum values found here are dependent of the time of simulation. In this manner, in Figs. 14, 16 it is shown the interval in which the controller can successfully reduce the e_{ss} for a ramp input. Lastly, it is important to notice that the controller can turn the system to a chaotic behaviour as shown in Fig. 17 due to the saturation of the system.

In conclusion, the discrete PID controller design using the sensitivity rules effectively controls the system for a step between $u \in [-0.25, 1.6]V$ and for a ramp input with a slope between $m \in [-0.03, 0.018]V/s$ approximately.

3) *Analytic design:* In this design, it is important to notice that even though the controller was designed with a reduced system which did not represent the system in a transitory state, as shown in [10], it accurately worked for designing this controller as shown in Figs. 19; this occurs because, this approximated system has some good properties that the original system does not possess but with some resemblance within the two. As shown in Fig. 20, the control action is barely not saturated as it is not passing the maximum value of the input 1500; in this manner, it is argued this is the upper bound for this controller as for more values it will start to saturate the system and not having a real action over it. On the other hand, for Fig. 21 it is seen the lower bound for this input, as for smaller values the system is saturated and the controller does not stabilize the system.

Lastly, the lower bound for the poles available are approximately 0.5 because, as shown in 22, if there are chosen a smaller poles than this value the controller cannot effectively stabilize the system and reduce the e_{ss} . This is easily explained the 0.4 poles are closer to the origin requiring a larger effort by the controller; in this manner, this effort saturates the system.

In conclusion, it was seen that the approximated system is useful to design a PID analytic controller with an interval for a step input of $u \in [-1.2, 1.5]V$ and for a chosen poles in $\text{poles} \in [0.5, 1]$. It is important to see that this controller has more range on the inputs that the design made by sensitivity.

B. Discrete state feedback controllers

1) $r(t) = 0$: This design made with the Ackerman method successfully controlled the system as shown in Fig. 23. This is expected to work very efficiently, as it was selected to be a dead beat controller therefore being the more fast possible control. The upper bound for a change in the initial conditions of the output was shown in Fig. 24 in which it is seen that the controller barely saturates the system; therefore, if this input would be larger the input would saturate the Rössler system. On the other hand, the lower bound for the initial condition of the output is 0, as it is a positive voltage in the system; in this manner, as shown in Fig. 25 it efficiently stabilizes the system in this lower bound.

In conclusion, it was found that the controller successfully stabilizes correctly the Rössler system for changes in the initial condition of the output for $\Delta x_3(0) \in [-2.6, 50]V$.

2) $r(t) \neq 0$: This state feedback controller was successfully designed to reduce the e_{ss} without saturating the system as shown in Fig. 26. In this case, it was expected for this controller to work as the selected poles were the same as the ones chosen in the discrete PID analytic controller; on the other hand, it similarly occurs that smaller poles do not control the system as it saturates the system. Continuing with this similarity, the upper bound is the same one as shown in Fig. 27 for the same reason. On the other hand, the lower bound found in Fig. 28 is smaller, therefore being a more accurate controller; this occurs because, the feedback controller has access to more information than the PID making it possible to control smaller inputs in this manner.

Lastly, in Fig. 29 it is seen that this controller, although it is capable to stabilize the system in a ramp, does not reduce the e_{ss} . This occurs because only one integrator was added to the system, therefore the e_{ss} for an input ramp is a constant value.

In conclusion, the state feedback discrete controller was successfully designed with an interval for an input of $u \in [-2, 1.5]V$. Furthermore, it can not reduce the e_{ss} for a ramp as it was only added one integrator to the plant.

An important remark, is that for every controller explained in this section the interval for the inputs are really close to the operation point; this happens because, the Rössler system has a chaotic behaviour for different parameters and inputs making it difficult to control.

C. Uncertainty Analysis

1) *Analytic Discrete PID Controller:* As seen in Figs. 31 and 30 for a 10% increase and decrease of the resistance R_a this controller successfully controls the system and reduces completely the stationary error without saturating the system. Then, the upper bound for the resistance a , as shown in Fig. 32 it is really high as for this value it barely saturates the system; in this manner, it is important to remark that the PID controller is highly robust as a controller designed for a value of a parameter works for a large margin of other values. Furthermore, in Fig. 33 a lower bound is found as for this value this controller makes it critically stable; this occurs because as found in [6] and [10], for smaller values of this resistance the system starts behaving chaotically making it difficult to control it.

In conclusion, the discrete PID controller is a very robust controller as it can reduce the e_{ss} for different margin of values for the $R_a \in [300, 2500]k\Omega$.

2) *State Feedback Controller $r(t) = 0$:* This controller does not work well for changes in the R_a , as shown in Figs. 35 and 34. This happens because this type of controller is only designed to work for this set of parameters, as this vector is the only one that is responsible for the controller; on the other hand, other controllers have different mechanisms that work together to ensure a robust control of the system. In this manner, this controller as it is such a minimalist one does not ensure control for similar systems varying the parameters. On the other hand, it is seen that this controller does stabilize the system in a quick way but not in 0, as it is desired.

In conclusion, this controller only stabilizes the system in 0 for the initial value of the resistance R_a , making it a not-robust controller different from the PID. It is important to notice that even if it uses more information than the PID, this controller has worse properties; so, the benefits of this controller are more on the side of having changes in the initial conditions instead of other values.

3) *State Feedback Controller $r(t) \neq 0$:* As presented in Figs. 36-37 (changes of 10%, this controller behaves properly, eliminating steady-state error for the predefined reference $r(t) = 1$). It is important to mention that this controller can still work really well for R_a around $3000k\Omega$ (as Fig. 38), where the system responds with no steady-state error but

showing a negative overshoot. Note that for significant a larger change downwards ($R_a = 250k\Omega$, Fig. 39), the system shows undesired behavior and cannot be accounted for a correct controller. In conclusion, just as the discrete PID controller designed, the state feedback controller shows robust behavior, working properly for resistors $R_a \in [450, 3000]k\Omega$.

V. CONCLUSIONS

In this work, a linear control to the Rössler circuit proposed by [5] was successfully designed with the procedures presented in section II, and then tested under different conditions. Although, some approaches (Ziegler-Nichols and Chien-Hrones-Reswick) did not provide good approximations for the discrete PID controller, the sensitivity and analytic methods showed proper behavior for certain intervals of the inputs and the R_a parameter, usually with an upper bound of $u_{ub} = 1.5$ and $R_a = 3000$, achieving absolute stability and eliminating steady-state error for a step and ramp input.

REFERENCES

- [1] O. E. Rössler, "An equation for continuous chaos," *Physics Letters A*, vol. 57, no. 5, pp. 397–398, 1976.
- [2] M. K. Mandal, M. Kar, S. K. Singh, and V. K. Barnwal, "Symmetric key image encryption using chaotic rossler system," *Security and Communication Networks*, vol. 7, no. 11, pp. 2145–2152, 2014.
- [3] D. S. Laiphrakpam and M. S. Khumanthem, "Cryptanalysis of symmetric key image encryption using chaotic rossler system," *Optik-International Journal for Light and Electron Optics*, vol. 135, pp. 200–209, 2017.
- [4] J. Weule *et al.*, "Detection of n: m phase locking from noisy data: application to magnetoencephalography," *Phys. Rev. Lett.*, vol. 81, no. 15, pp. 3291–3294, 1998.
- [5] V. Canals, A. Morro, and J. L. Rosselló, "Random number generation based on the rossler attractor," *IEICE Proceeding Series*, vol. 1, pp. 272–275, 2014.
- [6] J. S. Cárdenas and D. Plazas, "Simulation and analysis of chaotic rössler system based on circuits," 2019.
- [7] K. Ogata, *Modern Control Engineering*. Pearson, 2010.
- [8] C. M. Vélez, Control PID. [Online]. Available: <https://sci-ciencia.blogspot.com/2018/12/diapositivas-control-pid.html>
- [9] J. Ackermann, "Multi-model approaches to robust control system design," in *Uncertainty and Control*. Springer, 1985, pp. 108–130.
- [10] J. S. Cárdenas and D. Plazas, "Linear analysis of rössler system based on circuits," 2019.